Original research

Obesity-associated deficits in inhibitory control are phenocopied to mice through gut microbiota changes in one-carbon and aromatic amino acids metabolic pathways

María Arnoriaga-Rodríguez [1,2,3,4] Jordi Mayneris-Perxachs [1,2,3]
Oren Contreras-Rodríguez [2,5] Aurelijus Burokas [6,7]
Juan-Antonio Ortega-Sanchez,[6] Gerard Blasco,[8,9] Claudia Coll,[10] Carles Biarnés,[9]
Anna Castells-Nobau,[1,2,3] Josep Puig,[4,8,9] Josep Garre-Olmo,[4,11] Rafel Ramos [4,12]
Salvador Pedraza,[4,9,13] Ramon Brugada [4,14,15,16] Joan C Vilanova [4,9,13]
Joaquín Serena,[4,17] Jordi Barretina,[18] Jordi Gich,[4,19] Vicente Pérez-Brocal,[20,21]
Andrés Moya [20,21] Xavier Fernández-Real,[22] Lluis Ramio-Torrentà [4,10,17,19,23]
Reinald Pamplona,[24] Joaquim Sol,[24,25,26] Mariona Jové [24] Wifredo Ricart,[1,2,3,4]
Manuel Portero-Otin,[24] Rafael Maldonado,[6,27] Jose Manuel Fernández-Real [1,2,3,4]

Check for updates

ABSTRACT

Background Inhibitory control (IC) is critical to keep long-term goals in everyday life. Bidirectional relationships between IC deficits and obesity are behind unhealthy eating and physical exercise habits.

Methods We studied gut microbiome composition and functionality, and plasma and faecal metabolomics in association with cognitive tests evaluating inhibitory control (Stroop test) and brain structure in a discovery (n=156), both cross-sectionally and longitudinally, and in an independent replication cohort (n=970). Faecal microbiota transplantation (FMT) in mice evaluated the impact on reversal learning and medial prefrontal cortex (mPFC) transcriptomics.

Results An interplay among IC, brain structure (in humans) and mPFC transcriptomics (in mice), plasma/faecal metabolomics and the gut metagenome was found. Obesity-dependent alterations in one-carbon metabolism, tryptophan and histidine pathways were associated with IC in the two independent cohorts. Bacterial functions linked to one-carbon metabolism (*thyX,dut,* exodeoxyribonuclease V), and the anterior cingulate cortex volume were associated with IC, cross-sectionally and longitudinally. FMT from individuals with obesity led to alterations in mice reversal learning. In an independent FMT experiment, human donor's bacterial functions related to IC deficits were associated with mPFC expression of one-carbon metabolism-related genes of recipient's mice.

Conclusion These results highlight the importance of targeting obesity-related impulsive behaviour through the induction of gut microbiota shifts.

INTRODUCTION

Executive function constitutes one of the six key domains of cognition and mainly comprises

Summary box

What is already known on this subject?
► Inhibitory control is fundamental to keep long-term goals in everyday life.
► In subjects with obesity, this cognitive domain is impaired.

What are the new findings?
► Gut microbiome composition and functionality was linked to several tests evaluating inhibitory control in subjects with and without obesity.
► Brain structures associated with this cognitive domain was also associated with gut microbiome alterations.
► The impairment of inhibitory control from the donors was phenocopied in recipient mice through a faecal microbiota transplantation, resulting in alterations of reversal learning and changes in brain transcriptomics.

How might it impact on clinical practice in the foreseeable future?
► The adherence to diet could be improved by modifications in the gut microbiome.

reasoning, problem solving and component skills management, required for real-world adaptive success.[1] Executive functions are critical to keep long-term goals in everyday life.[2] Detrimental effects of excess weight on executive functions determine the individual's ability to break ingrained actions such as unhealthy eating and physical exercise habits in obese conditions.[3] Very preliminary small studies showed impaired executive function linked to the gut microbiota composition, suggesting that

the deleterious effects of adiposity on cognition are not merely mediated by the metabolic complications.[4]

We here aimed to study the interplay among IC, brain structure (in humans) and medial prefrontal cortex (mPFC) transcriptomics (in mice), plasma/faecal metabolomics and the gut metagenome and their transmission to mice through microbiota transplantation.

MATERIALS AND METHODS
Clinical study

Discovery cohort, cohort 1 (Ironmet): this is a cross-sectional case-control study setting at the Endocrinology Department of Josep Trueta University Hospital. The recruitment of subjects started in January 2016 and finished in October 2017. Consecutive middle-aged subjects, 27.2–66.6 years, were included. Patients with obesity (body mass index (BMI) ≥30 kg/m²) and age-matched and sex-matched subjects without obesity (BMI 18.5–<30 kg/m²), were eligible. Exclusion criteria were type 2 diabetes mellitus, chronic inflammatory systemic diseases, acute or chronic infections in the previous month; use of antibiotic, antifungal, antiviral or treatment with proton pump inhibitors; severe disorders of eating behaviour or major psychiatric antecedents; neurological diseases, history of trauma or injured brain, language disorders and excessive alcohol intake (≥40 g OH/day in women or 80 g OH/day in men).

Longitudinal cohort (Ironmet study): cognitive tests and MRI variables were collected again in 69 consecutive subjects after 1 year of follow-up.

Replication cohort, cohort 2: the study participants were recruited to evaluate the role of intestinal microflora in non-alcoholic fatty liver disease. The cohort included 24 subjects, 12 participants with obesity (BMI ≥30 kg/m²) and 12 without obesity (BMI <30 kg/m²). The exclusion criteria were systemic diseases, infection in the previous month, serious chronic illness, ethanol intake >20 g/day or use of medications that might interfere with insulin action. All control subjects were normotensive and were selected on the basis of similarity in age and sex compared with subjects with obesity and the absence of a personal history of inflammatory diseases or current drug treatment.

Replication cohort, cohort 3 (Imageomics): the Ageing Imageomics Study is an observational study including participants from two independent cohort studies (MESGI50 and MARK). Detailed description of the cohorts can be found elsewhere.[5] Briefly, the MESGI50 cohort included a population aged ≥50 years, while the MARK cohort included a random sample of patients aged 35–74 years with intermediate cardiovascular risk. Elegibility criteria included age ≥50 years, dwelling in the community, no history of infection during the last 15 days, no contraindications for MRI and consent to be informed of potential incidental findings.

Clinical and laboratory parameters: body composition was assessed using a dual energy X-ray absorptiometry (GE lunar, Madison, Wisconsin). Fasting plasma glucose, lipids profile and high-sensitivity C reactive protein (hsCRP) levels were measured using an analyzer (Cobas 8000 c702, Roche Diagnostics, Basel, Switzerland). Glycated haemoglobin was determined by performance liquid chromatography (ADAMA1c HA-8180V, ARKRAY, Kyoto, Japan).

Study of insulin sensitivity: Insulin sensitivity was determined by the hyperinsulinemic euglycemic clamp. The procedure consists in create in fasting conditions, a hyperinsulinemic state with an insulin infusion of predetermined fixed dosage and a variable rate glucose infusion. Glucose levels should be maintained constant at normal fasting (5 mmol/L) or any pre-existing (isoglycaemic) level adjusting the infusion rate of a 20% glucose solution. A steady state is usually reached in the last 40 minutes after 2 hours. Under these conditions the glucose infusion rates equal the glucose disposal rate, M (µmol· kg-1· min-1), a measurement of overall insulin sensitivity.

Dietary pattern: the dietary characteristics of the subjects were collected in a personal interview using a validated food-frequency questionnaire.[6]

The MRI acquisition and image preprocessing, the cognitive assessment (through the Stroop Color and Word Test (SCWT), Iowa Gambling Task (IGT) and the Wisconsin Card Sorting Test (WCST)), the extraction of faecal genomic DNA and whole-genome shotgun sequencing, plasma metabolomics analyses and animal experiments, including transcriptomics of the mPFC are described as online supplemental methods.

Statistical analyses

First, normal distribution and homogeneity of variances were tested. Results are expressed as number and frequencies for categorical variables, mean and SD for normal distributed continuous variables and median and IQR for non-normal distributed continuous variables. To determine differences between study groups, we used χ^2 for categorical variables, unpaired Student's t-test in normal quantitative and Mann-Whitney U test for non-normal quantitative variables. Spearman's analysis was used to determine the correlation between quantitative variables. All statistical analyses were performed with SPSS, V.19 (SPSS, Chicago, Illinois, USA).

Differential abundance analyses for taxa and Kyoto Encyclopedia of Genes and Genomes (KEGG)-based metagenome functions associated with the SCWT, the anterior cingulate cortex (ACC) volume and the recipient's mice mPFC gene transcripts were performed using the DESeq2 R packages, controlling for age, sex and education years. Fold change (FC) associated with a unit change in the corresponding variable and Benjamin-Hochberg adjusted p values were plotted for each taxon. Significantly different taxa were coloured according to phylum. Taxa and bacterial functions were previously filtered so that only those with >10 reads in at least two samples were selected. Manhattan-like plot were used to show significantly expressed KEGG metagenome functions. The $-\log_{10}(pFDR)$ values were multiplied by the FC sign to take into account the direction of the association. Bars were coloured according to the pFDR. A significance <0.05 was established unless otherwise indicated. DESeq2 was also used to identify recipient's mice mPFC genes associated with donor's metagenomic functions linked to the SCWT test controlling for donor's age, sex and education years. Gene Ontology (GO) and Reactome pathway analyses of differentially expressed genes were performed using the clusterProfiler R package[7] and the ConsensusPathDB,[8] respectively. The p value of each term was assessed using an hypergeometric test and significantly enriched terms were determined based on a q value (Storey correction) cut-off of 0.1, to account for multiple testing. GO terms were visualised using the goplot function from the enrichplot R package, and significant reactome pathways were visualised using a gene overlap plot.

Metabolomics data were analysed using machine learning (ML) methods. In particular, we adopted an all-relevant ML variable selection strategy applying a multiple random forest (RF)-based method as implemented in the Boruta algorithm.[9] It has been

Table 1 Clinical and neuropsychological data of the human discovery cohort

	Total population (n=114)	Without obesity (n=51)	With obesity (n=63)	P value
Age (years)	50.4 (41.8–58.6)	53.9 (44.4–59.0)	48.6 (40.7–57.5)	0.096
Females n (%)	79 (69.3)	34 (66.7)	45 (71.4)	0.584
Education (years)	12.5 (11–17)	15 (12–17)	12 (9–14)	1.9×10^{-5}
BMI (kg/m^2)	34.6 (25.3–43.3)	24.9 (2.6)	43.1 (6.7)	6.8×10^{-33}
Waist (cm)	110 (92–126)	89.8 (9.6)	125.5 (14.0)	5.8×10^{-29}
Fat mass (%)	43.5 (33.8–50.2)	32.4 (7.2)	49.7 (5.5)	2.7×10^{-24}
SBP (mmHg)	132.8 (20.2)	124.3 (15.8)	139.5 (20.9)	2.6×10^{-5}
DBP (mmHg)	74.8 (11.6)	71.2 (10.9)	77.7 (11.4)	0.003
HDL-C (mg/dL)	56 (45–68)	66.0 (17.0)	51.0 (12.9)	4.1×10^{-7}
Triglycerides (mg/dL)	90.5 (65.8–135.3)	79 (58–96)	124 (82–156)	4.0×10^{-5}
FPG (mg/dL)	96 (90–103)	95 (89–101)	97 (93–105)	0.155
HbA1c (%)	5.5 (0.3)	5.5 (5.3–5.6)	5.6 (5.3–5.8)	0.021
hsCRP (mg/dL)	1.8 (0.7–5.9)	0.7 (0.4–1.3)	4.9 (2.7–9.5)	1.6×10^{-13}
SCWT (score)	43.1 (10.1)	45.9 (9.6)	40.8 (10.0)	0.006

Results are expressed as number and frequencies for categorical variables, mean and SD for normal distributed continuous variables and median and IQR for non-normal distributed continuous variables. To determine differences between study groups, we used χ^2 for categorical variables, unpaired Student's t-test in normal quantitative and Mann-Whitney U test for non-normal quantitative variables. P value determines differences between subjects with obesity (BMI ≥30 kg/m^2) and without obesity (BMI 18.5–30 kg/m^2). BMI, body mass index; DBP, diastolic blood pressure; FPG, fasting plasma glucose; HbA1c, glycated haemoglobin; HDL-C, high-density lipoprotein cholesterol; hsCRP, high-sensitivity C reactive protein; SBP, systolic blood pressure; SCWT, Stroop Color and Word Test.

recently proposed as one of the two best-performing variable selection methods making use of RF for high-dimensional omics datasets.[10] The Boruta algorithm is a wrapper algorithm that performs feature selection based on the learning performance of the model.[9] It performs variables selection in three steps: (a) randomisation, which is based on creating a duplicate copy of the original features randomly permutate across the observations; (b) model building, based on RF with the extended data set to compute the normalised permutation variable importance measure (VIM) scores; (c) statistical testing, to find those relevant features with a VIM higher than the best randomly permutate variable using a Bonferroni corrected two-tailed binomial test and (d) iteration, until the status of all features is decided. We run the Boruta algorithm with 500 iterations, a confidence level cut-off of 0.005 for the Bonferroni adjusted p values, 5000 trees to grow the forest (*ntree*) and a number of features randomly sampled at each split given by the rounded down number of features/3 (the *mtry* recommended for regression).

RESULTS AND DISCUSSION
We initially evaluated the SCWT in a cohort of subjects with and without obesity. As expected, lower SCWT scores, indicative of impaired inhibitory control, were found in subjects with obesity (table 1, figure 1A). Inhibitory control was associated with the gut microbiota composition. Differential abundance of species associated with the SCWT were identified from raw read count data adjusted by age, sex and education years using the DESeq2 package in R. We identified 297 species (*p*FDR <0.1) associated with the SCWT (figure 1A; online supplemental table S1). In all subjects as a whole, positive associations with executive performance were found with *Eubacterium* sp *CAG:603* and *Firmicutes bacterium CAG:238*; whereas most of the species negatively linked to SCWT scores belonged to the Bacteroidetes phylum: *Bacteroides plebeius*, *Bacteroides gallinarum*, *Bacteroides mediterranensis*, *Desulfovibrio fairfieldensis*, *Lachnospiraceae bacterium 5_1_57FAA* and *Lachnospiraceae bacterium 6_1_37FAA*. As both inflammation and insulin resistance may play a role in cognitive function and neurodegenerative disorders, we further analysed the data controlling for hsCRP, a marker of inflammation, and

the hyperinsulinaemic-euglycaemic clamp (he-clamp), the gold-standard method to assess insulin sensitivity. Notably, ~85% of the species associated with the SCWT were still significant after adjusting for both parameters. We could reproduce these results in an independent cohort (n=24) (table 2) using two measures of executive function (the IGT and the WCST): several *Bacteroides* sp and *Alistipes* sp were also associated with the scores of these tests (figure 1B, online supplemental figure S1A, online supplemental tables S2 and S3).

Metagenome functional analyses based on KEGG pathways controlling for age, sex and education years also revealed significant associations of several bacterial pathways with the SCWT (figure 1C, online supplemental table S6), which were also replicated in an independent cohort (figure 1D). Further analysis controlling for hs-CRP and he-clamp revealed no effect of either inflammation or insulin sensitivity. Thus, >98% of the species associated with the SCWT were still significant after controlling for these additional variables. Notably, three bacterial functions related to nucleotide metabolism (dUTP pyrophosphatase, *dut*; thymidylate synthase, *thyX* and exodeoxyribonuclease V) had the strongest negative associations with the SCWT. Both *dut* and *thyX* participate in folate-mediated one-carbon metabolism. Consistently, *dut* correlated significantly with the plasma folic acid concentration (R=0.32, p=7×10^{-4}, online supplemental figure S1B). It could seem counterintuitive that plasma folic acid was positively associated with a function linked to worse cognitive function. However, circulating unmetabolised folic acid implies that the body's capacity to convert folic acid to the metabolically active 5-methyltetrahydrofolate has been overwhelmed and that folic acid has passively diffused intact into the circulation.[11] In addition, *thyX* had a negative correlation with plasma uric acid levels (R=−0.20, p=0.034, online supplemental figure S1C). Alterations in folate-mediated one-carbon metabolism have been associated with increased risk for cognitive decline.[11] In line with these findings, other functions related to folate-mediated one-carbon metabolism (phosphoribosylglycinamideformyltransferase 2, *purT*) or folate biosynthesis (2-amino-4-hydroxy-6-hydroxymethyldihydropteridine diphosphokinase, *folK*; dihydroneopterin triphosphate diphosphatase, *nudB*) were also negatively
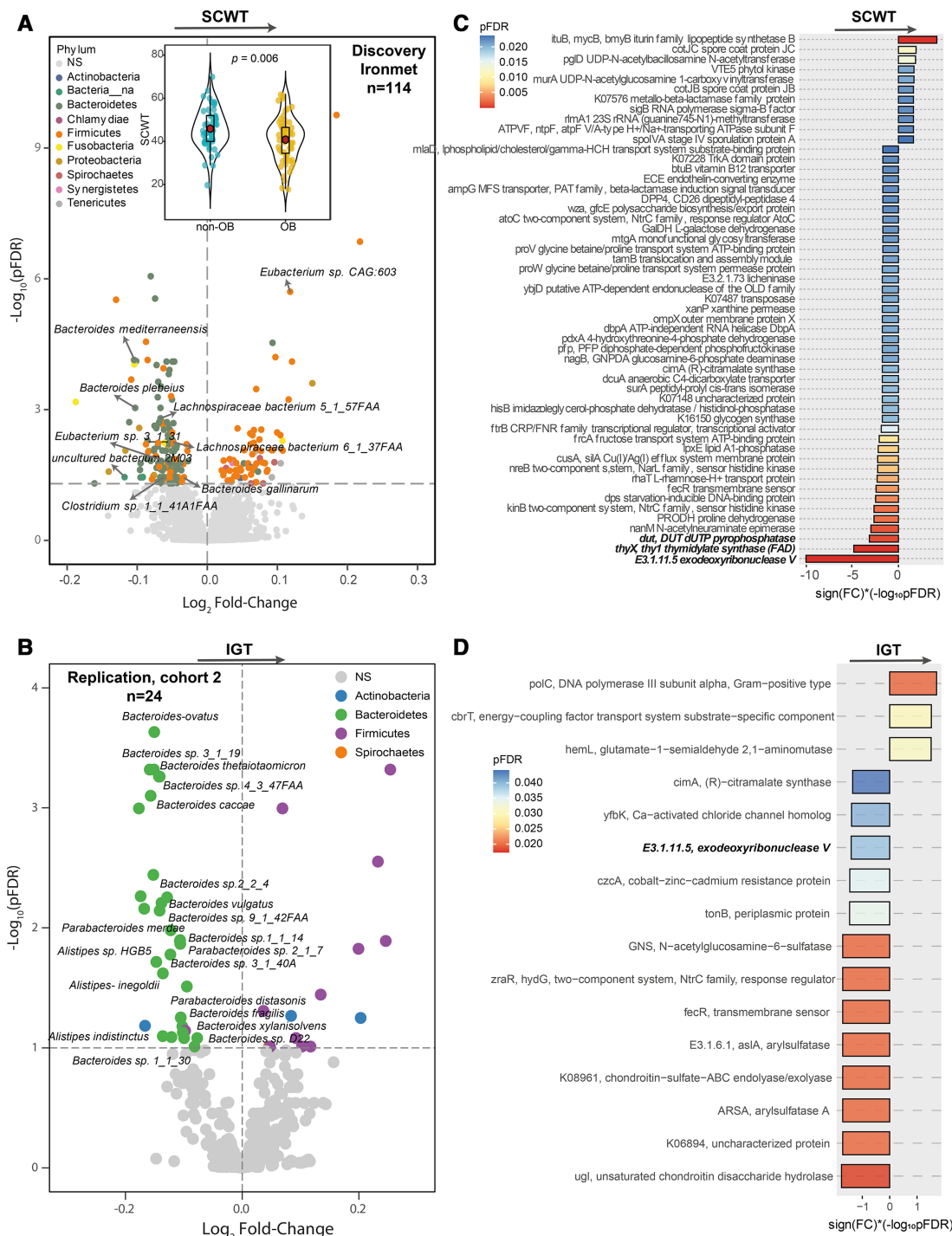
Figure 1 A microbiota taxonomic and functional signature is associated with inhibitory control. (A) Volcano plot of differential bacterial abundance (pFDR <0.05) associated with the Stroop Color Word Test (SCWT) as calculated by DESeq2 from shotgun metagenomic sequencing in the IRONMET cohort (n=114), adjusting for age, sex and education years. Fold change (FC) associated with a unit change in the SCWT and Benjamini-Hochberg adjusted p values (pFDR) are plotted for each taxon. Significantly different taxa are coloured according to phylum. In the same graph, the violin plots for the SCWT scores in patients with and without obesity are also shown. Differences between groups were analysed by a Wilcoxon tests. (B) Volcano plot of differential bacterial abundance (pFDR <0.1) associated with Iowa Gambling Test (IGT) as calculated by DESeq2 from shotgun metagenomic sequencing in an independent cohort (n=24), adjusting for age, sex and education years. (C) Manhattan-like plot of significantly expressed KEGG metagenome functions associated with the SCWT (pFDR <0.020) identified from DESeq2 analysis in the IRONMET cohort (n=114) adjusted for age, sex and educations. The −log$_{10}$(pFDR) values are multiplied by the FC sign to take into account the direction of the association. Bars are coloured according to the pFDR. (D) Manhattan-like plot of significantly expressed KEGG metagenome functions associated with the IGT (pFDR <0.05) identified from DESeq2 analysis in an independent cohort (n=24) adjusted for age, sex and educations.

Table 2 Clinical and neuropsychological data of the human replication cohort

	Total population (n=24)	Without obesity (n=12)	With obesity (n=12)	P value
Age (years)	53.5 (44.3–57.8)	52 (39–58.3)	53.5 (48.5–57.8)	0.478
Females n (%)	15 (62.5)	7 (58.3)	8 (66.7)	0.673
Education (years)	16 (15–17)	17 (14–17)	16 (15–17)	1.9×10^{-5}
BMI (kg/m^2)	29.9 (23.2–45.1)	23.2 (21.3–25.5)	44.3 (38.6–47.7)	3.2×10^{-5}
Waist (cm)	96 (81–127)	82 (72.8–87.8)	127 (121–136)	7.1×10^{-5}
Fat mass (%)	37.4 (29.2–45.3)	29.6 (21.3–34.9)	45.2 (39.6–51.3)	2.8×10^{-4}
SBP (mmHg)	123.5 (115–136.8)	116 (108–121.3)	135.5 (124.5–148.3)	0.001
DBP (mmHg)	69.5 (64.3–78.8)	64.5 (59.5–69.5)	78 (69.3–150.8)	0.003
HDL-C (mg/dL)	56 (43–76)	67 (58.3–77)	44.5 (40–52.8)	0.043
Triglycerides (mg/dL)	73 (48.8–117.5)	57.5 (42.3–98.5)	93 (68.5–150.8)	0.069
FPG (mg/dL)	94.5 (84–103.8)	92 (84–102)	99 (85.3–103.8)	0.418
HbA1c (%)	5.5 (5.3–5.8)	5.5 (5.3–5.7)	5.7 (5.3–6.3)	0.147
hsCRP (mg/dL)	0.2 (0–0.5)	0.1 (0–0.2)	0.5 (0.2–0.8)	0.009
IGT (score)	45 (42–49)	44.5 (39–48.3)	45.5 (43.3–49.8)	0.271
WCST (score)	11 (11–12)	11 (10.5–12.5)	11 (11–12)	0.918

Results are expressed as number and frequencies for categorical variables, mean and SD for normal distributed continuous variables and median and IQR for non-normal distributed continuous variables. To determine differences between study groups, we used χ^2 for categorical variables, unpaired Student's t-test in normal quantitative and Mann-Whitney U test for non-normal quantitative variables. P value determines differences between subjects with obesity (BMI ≥30 kg/m^2) and without obesity (BMI 18.5–30 kg/m^2). BMI, body mass index; DBP, diastolic blood pressure; FPG, fasting plasma glucose; HbA1c, glycated haemoglobin; HDL-C, high-density lipoprotein cholesterol; hsCRP, high-sensitivity C reactive protein; IGT, Iowa Gambling Test; SBP, systolic blood pressure; WCST, Wisconsin Card Sorting Test.

associated with the SCWT. In addition, several functions related to vitamins involved in the folate and one-carbon metabolism, specifically vitamin B$_6$ (4-hydroxythreonine-4-phosphate dehydrogenase, *pdxA*), vitamin B$_{12}$ (vitamin B$_{12}$ transporter, *btuB*) and vitamin B$_2$ (5,6-dimethylbenzimidazole synthase, *bluB*; 3,4-dihydroxy 2-butanone 4-phosphate synthase, *ribBA*; riboflavin synthase, *ribE*), were also negatively associated with the SCWT.

Notably, the associations between the SCWT and bacterial composition were different in subjects with and without obesity. Negative associations with *Bacteroides nordii*, *Fusobacterium varium*, *Prevotella* sp CAG:279 and *Prevotella timonensis* were observed in subjects with obesity, while *Bacteroides ovatus* CAG:22, *Bacteroides* sp CAG:462, *Alistipes* sp CAG:157, *Rikenellaceae* sp and *Acidaminococcus* sp were associated negatively in subjects without obesity (figure 2A,B, online supplemental tables S4 and S5). In the latter, we also observed positive associations with *Roseburia* sp CAG:471, *Clostridum* sp CAG:632, *Pasteurellaceae* sp and *Butyrivibrio* sp CAG:318. Similarly, the associations at the functional level were also different in subjects with and without obesity. In particular, the association of the SCWT with the one-carbon metabolism-related functions *thyX* and *dut* was specifically significant among individuals without obesity (figure 2C, online supplemental table S7), white the link with exodeoxyribonuclease V was prominent among subjects with obesity (figure 2D, online supplemental table S8). Remarkably, most of these metagenomic composition and functional associations were replicated longitudinally after 1 year of follow-up (online supplemental figure S1D,E and tables S9 and S10). In addition to exodeoxyribonuclease V, *dut*, *thyX* and *kinB*, the SCWT performance at follow-up had a relatively strong negative association with nicotinamide phosphoribosyltransferase. The knockdown of this gene in mice has shown to recapitulate hippocampal cognitive phenotypes in old mice.[12]

We then used a multiple RF models-based ML variable selection strategy, as implemented in the Boruta R package, to identify plasma and faecal metabolites predictive of the SCWT. Among the plasma metabolites positively associated with

SCWT performance, tryptophan and 4-hydroxyphenyllactic acid (4-HPLA, a tyrosine catabolite) were the most important (figure 3A,B). Tryptophan and tyrosine are the precursors for the synthesis of the neurotransmitters serotonin and dopamine, respectively. In healthy adults, low tryptophan levels were associated with a decrease in the Stroop interference effect,[13] [14] although the results are somewhat inconsistent.[15] [16] Previous research has also suggested that inhibitory control also relies on dopaminergic signalling.[17] Stimulation of dopamine D$_2$ receptors has shown to decrease Stroop interference.[18] A higher dopaminergic uptake was also linked to less WCST-related activation in the PFC.[19] Increased 4-HPLA acid levels may indicated that tyrosine is diverted from dopamine synthesis. Interestingly, 4-HPLA is a microbial-derived tyrosine catabolite that has shown to decrease reactive oxygen species production in both mitochondria and neutrophils.[20] Alterations in tryptophan and tyrosine metabolism in relation to SCWT performance were also observed in faecal samples (figure 3C,D). Hence, 5-hydroxyindoleacetic acid (5-HIAA), the end-product of serotonin metabolism, tyrosine itself and some microbial-derived tyrosine metabolites (2-phenylpropanoic acid) had consistent associations with the SCWT. The associations between the SCWT and alterations in tryptophan metabolism were replicated in the Imageomics cohort (n=970), where plasma levels of tryptophan and some microbial-derived tryptophan catabolites (indolepropionamide) were positively associated with the SCWT performance (figure 3F,G). Remarkably, these alterations in tryptophan metabolism were only observed in individuals with obesity in both the Ironmet (figure 4A-J) and Imageomics cohorts (figure 4K-M). This is in line with recent studies reporting alterations in tryptophan metabolic pathways in obesity in association with systemic inflammation.[21] A summary of these findings can be found in figure 5A.

The purine, thymidylate and methionine cycles encompass the one-carbon metabolism in the cytosol, which largely rely on B vitamins, specifically vitamins B$_2$, B$_6$, folate (B9) and vitamin B$_{12}$.[22] In agreement with alterations in the metagenomic functions involved in the two former cycles and one-carbon
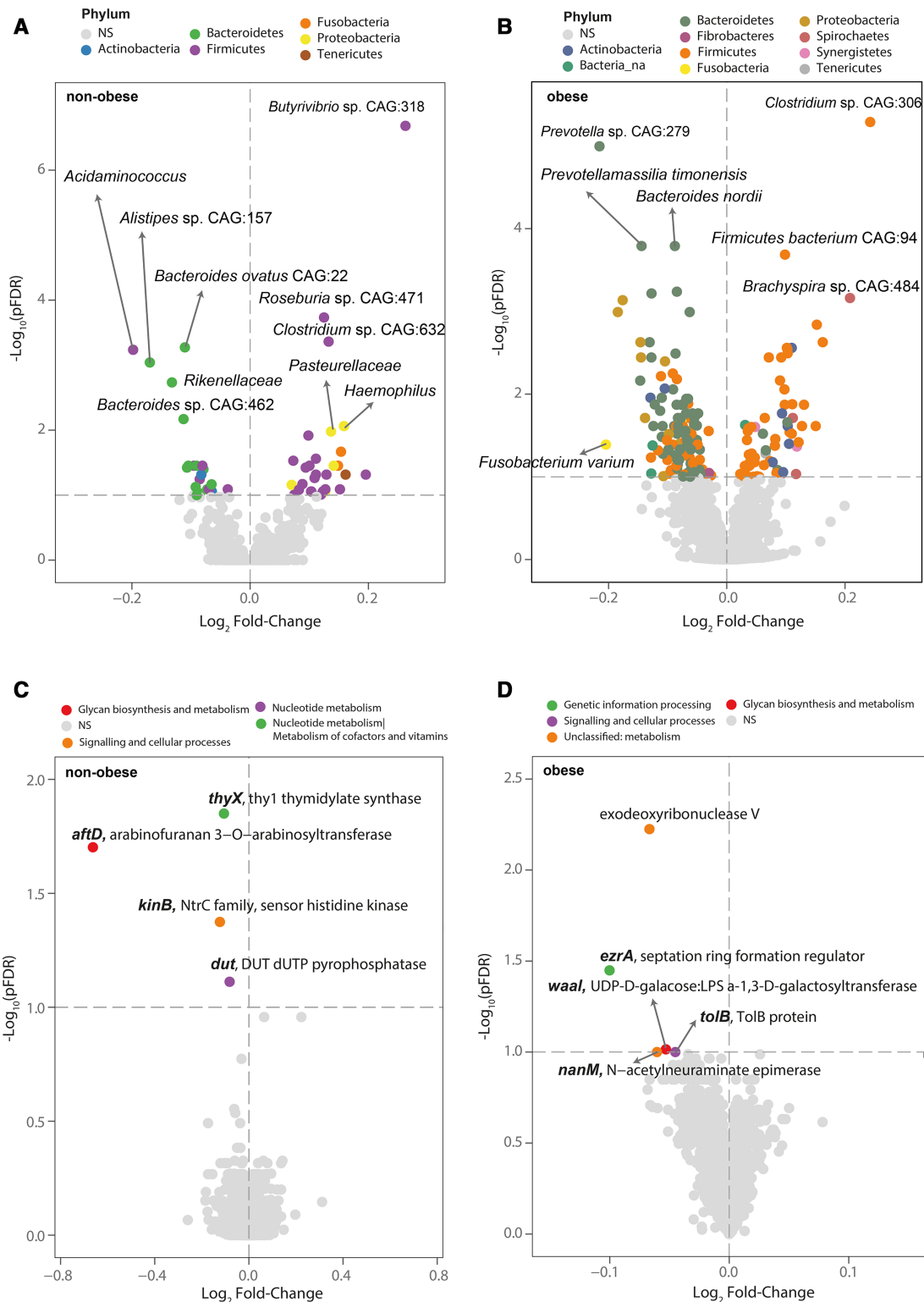
Figure 2 The microbiota taxonomic and functional signature linked to inhibitory control is modulated by obesity. (A, B) Volcano plot of differential expressed (pFDR <0.1) bacterial abundance and (C, D) bacterial functions associated with the Stroop Color and Word Test (SCWT) as calculated by DESeq2 from shotgun metagenomic sequencing in the patients without and with obesity from the IRONMET cohort, respectively, controlling for age, sex and education years. Fold change associated with a unit change in the SCWT and Benjamini-Hochberg adjusted p values (pFDR) are plotted for each taxon. Significantly different taxa are coloured according to phylum.

metabolism-related vitamins in relation to the SCWT scores, we found negative associations between the faecal levels of methionine and microbial-derived methionine catabolites (dimethyl sulfone)[23] in the Ironmet cohort (figures 3D,E and 5B).

Interestingly, these alterations in the methionine cycle were only observed in individuals without obesity (figure 4E-I), who also had alterations in betaine (figure 4E), which serves as a methyl donor in the reaction converting homocysteine to methionine
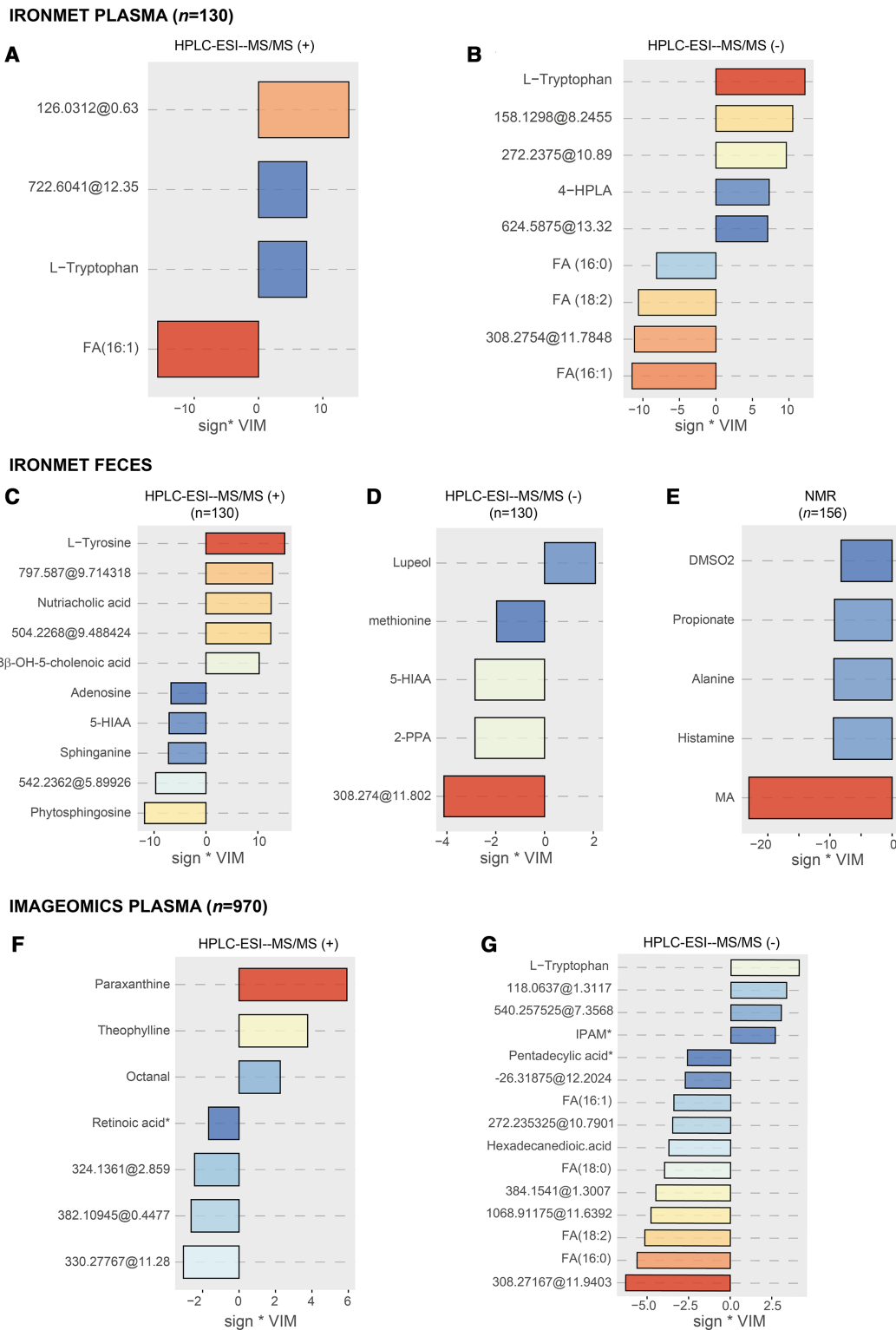
Figure 3 Plasma and faecal metabolomics linked to inhibitory control in the Ironmet and Imageomics cohorts. Bar plots of normalised variable importance measure (VIM) for the metabolites associated with the Stroop Color and Word Test (SCWT) in (A, B) plasma and (C–E) faecal samples identified by HPLC-ESI-MS/MS in positive mode (n=130), negative mode (n=130) and NMR (n=156), respectively, in the Ironmet cohort. Bar plots of VIM for the metabolites associated with the SCWT in plasma samples of the Imageomics cohort (n=970) identified by HPCL-ESI-MS/MS in (F) positive and (G) negative mode. In all cases, metabolites were identified using a multiple random forest-based machine learning variable selection strategy using the Boruta algorithm with 5000 trees and 500 iterations. All metabolites were identified based on exact mass, retention time and MS/MS spectrum, except those with (*) that were only identified based on exact mass and retention time. Unidentified metabolites are shown as exact mass at retention time. 2-PPA, 2-phenylpropanoic acid; 4-HPLA, 4-hydroxyphenyllactic acid; 5-HIAA, 5-hydroxyindoleacetic acid; DMSO2, dimethyl sulfone; FA, fatty acid; IPAM, indolepropionamide; MA, methylamine; TMA, trimethylamine.
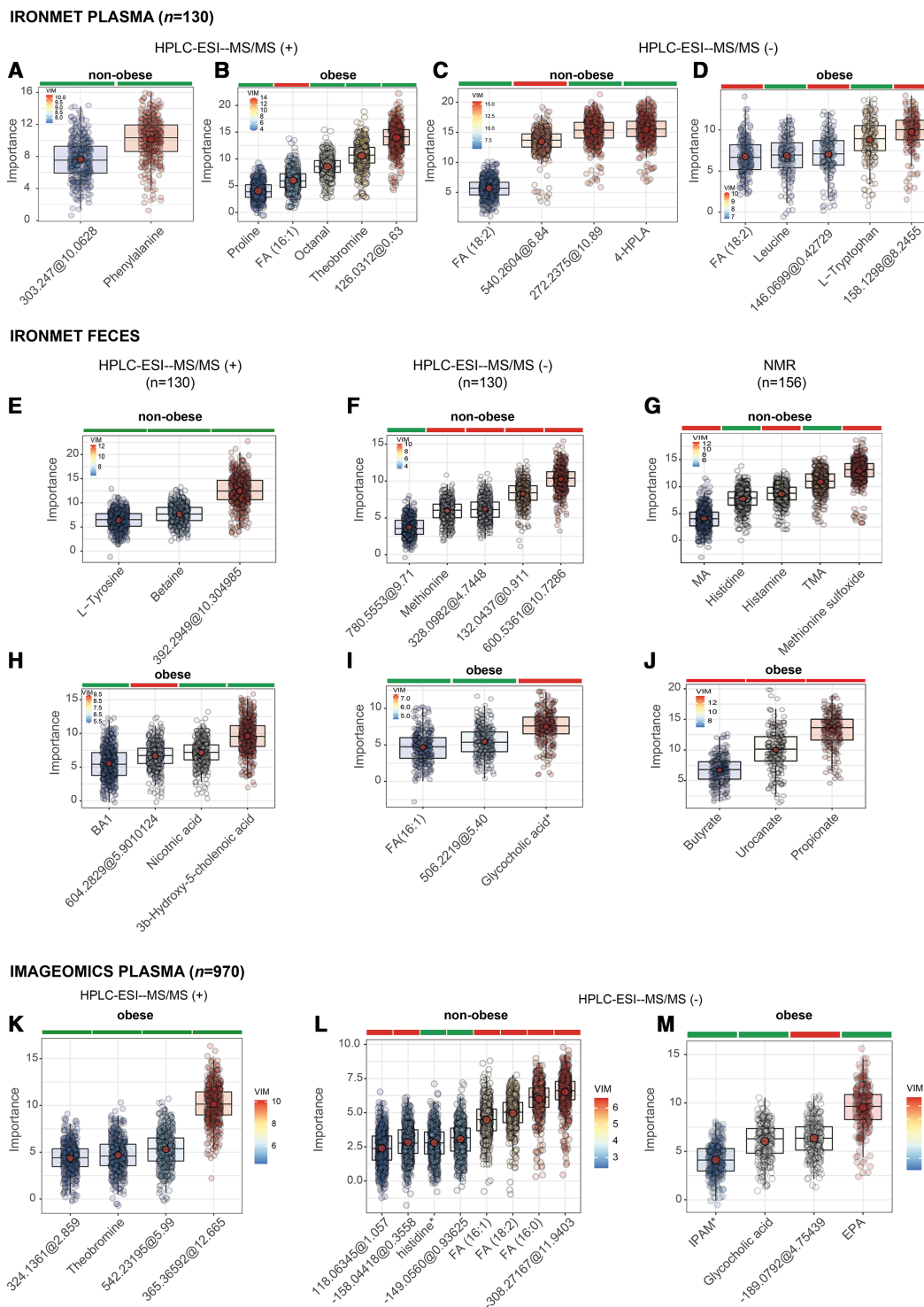
Figure 4 Plasma and faecal metabolomics linked to inhibitory control in the Ironmet and Imageomics cohorts according to obesity status. Bar plots of normalised variable importance measure (VIM) for the metabolites associated with the Stroop Color and Word Test (SCWT) in (A–D) plasma and (E–J) faecal samples identified by HPLC-ESI-MS/MS in positive mode (n=130), negative mode (n=130) and NMR (n=156), respectively, in the Ironmet cohort in patients with and without obesity. Bar plots of VIM for the metabolites associated with the SCWT in plasma samples of the Imageomics cohort (n=970) identified by HPCL-ESI-MS/MS in (K) positive and (L, M) negative mode in patients with and without obesity. The above colour bar indicates the sign of the association among the metabolites and the SCWT, with red indicating negative correlation and green positive correlation. In all cases, metabolites were identified using a multiple random forest-based machine learning variable selection strategy using the Boruta algorithm with 5000 trees and 500 iterations. All metabolites were identified based on exact mass, retention time and MS/MS spectrum, except those with (*) that were only identified based on exact mass and retention time. Unidentified metabolites are shown as exact mass at retention time. 4-HPLA, 4-hydroxyphenyllactic acid; BA1, Bile acid1: 4,4-dimethyl-5-α-cholesta-8,14-dien-3β-ol; EPA, eicosapentaenoic acid; FA, fatty acid; IPAM, indolepropionamide; MA, methylamine; TMA, trimethylamine.
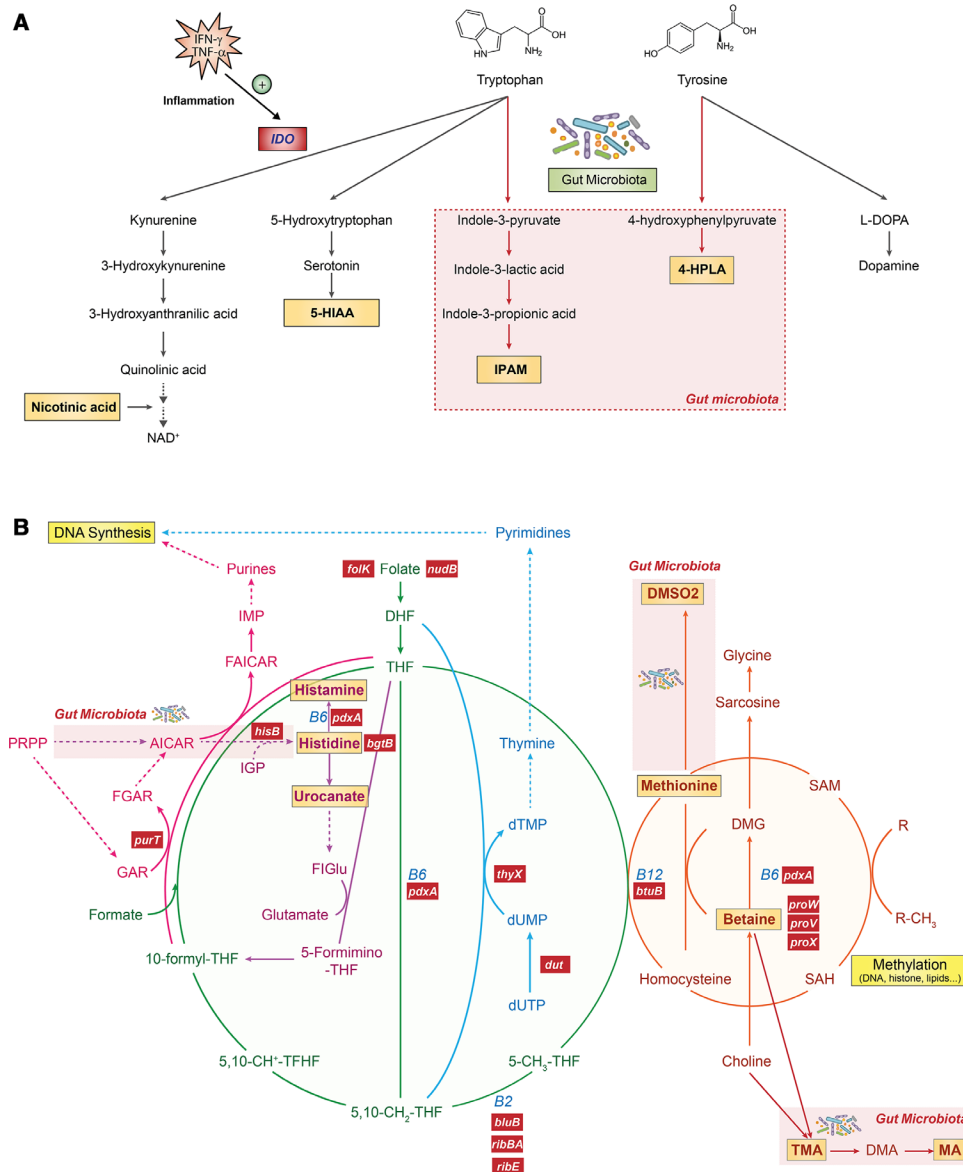
Figure 5 Main metabolic pathways involved in the associations among metagenomics, metabolomics and the Stroop Color and Word Test (SCWT). (A) Overview of the main catabolic pathways of tryptophan and tyrosine. Tryptophan and tyrosine are the precursors for the synthesis of the neurotransmitters serotonin and dopamine, respectively. The gut microbiota can also metabolise tryptophan and tyrosine to indoles and hydroxyphenolic acids, respectively. Dietary tryptophan is mostly metabolised via the Kynurenine pathway, which is activated by inflammation. (B) Overview of the folate-mediated one-carbon metabolism. The folate cycle (green) is required for the synthesis of DNA (pink and blue) as well as methylation reaction (DNA, proteins and lipids) through the methionine cycle (orange). Histidine (purple), choline and betaine are two sources of 1C units feeding into the one-carbon metabolism. Bacterial pathways have been shaded in red. Metabolites involved in the one-carbon metabolism and significantly associated with the SCWT are highlighted in bold in a yellow box. Bacterial functions participating in the one-carbon metabolism and significantly associated with the SCWT are highlighted in bold in a red box. AICAR, 5-aminoimidazole-4-carboxamide 1-β-D-ribofuranoside; *bgtB*, arginine/lysine/histidine/glutamine transport system substrate-binding and permease protein; *bluB*, 5,6-dimethylbenzimidazole synthase; *btuB*, vitamin B$_{12}$ transporter; DHF, dihydrofolate; DMA, dimethylamine; DMSO2, dimethylsulfone; *dut*, dUTP pyrophosphatase; FAICAR, 5-formamidoimidazole-4-carboxamide ribotide; FGAR, 5′-phosphoribosyl-N-formylglycineamide; FIGlu, N-Formimino-glutamate; *folK*, 2-amino-4-hydroxy-6-hydroxymethyldihydropteridine diphosphokinase; GAR, 5′-phosphoribosylglycineamide; *hisB*, imidazoleglycerol-phosphate dehydratase; IGP, imidazole glycerol-phosphate; IMP, inosine 5′-monophosphate; MA, methylamine; *nudB*, dihydroneopterin triphosphate diphosphatase; *pdxA*, 4-hydroxythreonine-4-phosphate dehydrogenase; *proV*, glycine betaine/proline transport system ATP-binding protein; *proW*, glycine betaine/proline transport system permease protein; *proX*, glycine betaine/proline transport system substrate-binding protein; *purT*, phosphoribosylglycinamide formyltransferase 2; *ribBA*, 3,4-dihydroxy 2-butanone 4-phosphate synthase/GTP cyclohydrolase II; *ribE*, riboflavin synthase; SAH, S-adenosylhomocysteine; SAM, S-adenosylmethionine; THF, tetrahydrofolate; *thyX*, thymidylate synthase; TMA, trimethylamine.

(figure 5B). These results are in agreement with the observed associations among one-carbon metabolism related metagenomic functions (*thyX* and *dut*) and SCWT only in individuals without obesity. These alterations in betaine levels are also consistent with the significant associations between the SCWT and bacterial betaine transport functions (*proW*, betaine/proline transport system permease protein; *proV* betaine/proline transport system ATP-binding protein; *proX*, betaine/proline transport

system substrate-binding protein) (online supplemental table S6, figure 5B). It is also worth noting that both betaine and its precursor (choline) can be metabolised by the gut microbiota to trimethylamine (TMA) and eventually methylamine (MA), which were also only associated with the SCWT in individuals without obesity (figure 4G).

Another one-carbon donor that contributes to the pool of 1C units in the folate-bound one-carbon metabolism is histidine (figure 5B).[24] Again, in agreement with the above findings, plasma histidine was positively associated with SCWT in individuals without obesity in the Imageomics cohort (figure 4L). Histidine is an important precursor of histamine, which acts as a neurotransmitter in the brain and has been involved in anxiety, stress response, learning and memory.[25] Consistently, we also found negative associations between faecal histamine and SCWT (figure 4G). Notably, vitamin B_6 acts as a cofactor for histidine decarboxylase, the sole enzyme responsible for the conversion of histidine to histamine. Histidine can alternatively be converted to urocanic acid, which was significantly associated with the SCWT performance in individuals with obesity (figure 4J). Urocanate has recently shown to cross the blood-brain barrier and promote glutamate biosynthesis and release in various brain regions, thereby enhancing learning and memory.[26] Therefore, histidine might be metabolised differently in obesity.

We further analysed the associations among the metabolome and those bacterial functions most negatively associated with the SCWT. ML analyses revealed consistent associations with tryptophan, 4-HPLA, 3-methyl-2-oxovalerate, FA(16:1) and FA(18:2) (online supplemental figure S2 A–C). These functions also had positive associations with betaine, reflecting the involvement of these functions in the one-carbon metabolism.

We next questioned whether these associations could have a structural correlate. Both the anterior cingulate and the PFC are thought to be critically involved in the performance of the Stroop task. In agreement with previous findings,[27] we found that the grey matter volume of the ACC was positively linked to SCWT scores (figure 6A,B). Interestingly, in line with inhibitory control-bacterial relationships, we found negative associations of different *Bacteroides* sp, *Anaerovibrio* sp RM50 and *Selenomonas* sp *Oral taxon 478* with ACC volume (figure 6C, online supplemental table S11). Conversely, bacterial species positively associated with better inhibitory control were also directly linked to ACC volume (*Clostridium* sp CAG:226, *Roseburia* sp CAG:182 and *Ruminococcus* sp CAG:417). The strongest negative associations between the bacterial functions and the ACC volume were with *kinB*, *dut* and *thyX*, that were precisely the bacterial function negatively associated with SCWT in subjects without obesity (figure 6D). Other bacterial functions involved in pyrimidine metabolism were positively linked (pseudouridylate synthase, *psuG*; TYMP thymidine phosphorylase, *deoA*; 5'-deoxynucleotidase, *yfbR*) (figure 6D,E, online supplemental table S12). An increased frequency of red meat consumption was associated with those bacterial functions negatively related to inhibitory control (online supplemental figure S3A). Of note, *dut* and *kinB* had the strongest negative associations with the ACC volume at baseline, and after 1 year of follow-up (online supplemental figure S3B).

The correlates of cognitive flexibility of humans and mice are often measured using reversal learning (RL) paradigm experiments, in which subjects need to overcome established associations and learn new ones based on feedback.[28] RL also provides a measure of inhibition and impulsiveness.[29] In a faecal microbiota transplantation experiment, microbiota from n=22 humans donors (n=11 with BMI <30 kg/m² and n=11 with BMI ≥30

kg/m² matched for age, sex and education years) was orally delivered to recipient mice (figure 7A, online supplemental table S13). Mice receiving the microbiota from the subjects with obesity with lower inhibitory control had significantly lower RL performance at day 18 evaluated as the number of lever-presses in the inverted active lever (figure 7A). Remarkably, several human donor's bacterial species (figure 7B, online supplemental table S1) and functions (figure 7C, online supplemental table S6) associated with the SCWT in humans were also associated with the recipient's mice RL task performance.

PFC activity is known to affect inhibitory control, and inhibitory control-related activity in regions of the PFC have been found to correlate inversely with BMI and weight increase.[30 31] Therefore, in an independent faecal microbiota transplantation experiment, we performed an RNA sequencing of the mPFC of mice that received microbiota from human donor's with either low or high SCWT scores matched for age, gender and education years (figure 7D, online supplemental table S14). DESeq2 analyses adjusted for donor's age, sex and education years, revealed several mPFC genes from recipient's mice associated with the SCWT-related human's donor bacterial functions (figure 7E,F, online supplemental table S15 and S16). In particular, *dut* had significative positive associations with the expression of *Kcne2*, *Prlr*, *Folr1*, *Cldn2*, *Slc4a5*, *Sostdc1* and borderline associations (pFDR <0.11) with *Tmem72*, *F5* and *Ttr* (figure 7E). Remarkably, all these genes were found among the top 25 genes changing the hippocampal expression after contextual fear conditioning.[32] Enrichment analysis of differentially expressed genes based on GO revealed over-representation of biological processes related to neuron development and histone methylation (online supplemental figure S4A). The genes involved in these processes included *Folr1*, *Mecp2*, *Auts2*, *Mfrp* and *Hipk1*. It is particularly noticeable, the significant association between this donor's bacterial function involved in folate-mediated one-carbon metabolism and the expression of the folate receptor 1 (*Folr1*) and methyl-CpG binding protein 2 (*Mecp2*) in the recipient mice mPFC. This is in agreement with our previous findings and further highlights the key role of the one-carbon metabolism and its involvement in DNA methylation. The *Mecp2* has a well-established function in neurodevelopment[33] and has also been linked to autism and Alzheimer's disease.[34] On the other hand, exodeoxyribonuclease V was significantly associated with the expression of 152 PFC genes, with transthyretin having the strongest FC by far (figure 7F). Ttr is one of the major amyloid β peptide-binding proteins acting as a neuroprotector in Alzheimer's disease.[35] This bacterial function also had a significant association with methylenetetrahydrofolate dehydrogenase 1-like (*Mthfd1l*) gene, which encodes for an enzyme that has an important role in folate-mediated one-carbon metabolism. Deletion of one allele of *Mthfd1* resulted in impaired cue-conditional learning in mice.[36] Finally, enrichment analyses based on reactome pathways revealed a network of pathways related to netrin signalling, which has recently shown to play an important role in synaptic plasticity and memory formation.[37]

Next, we also searched for relevant genes in the PFC of recipient's mice that were able to predict the human's donor SCWT using an ML-based variable selection strategy. After application of the Boruta algorithm, we identified *Ms4a4a* and the monocarboxylic acid transporter 12 (*Slc16a12*) as the main predictors of SCWT (figure 7G). Interestingly, the later gene has been recently described to be linked to folate status.[38] Monocarboxylate transporter transports lactate to the brain and promotes neurogenesis.[39] In addition, this is the transporter for creatine. Spontaneous mutations in creatine transporters and creatine
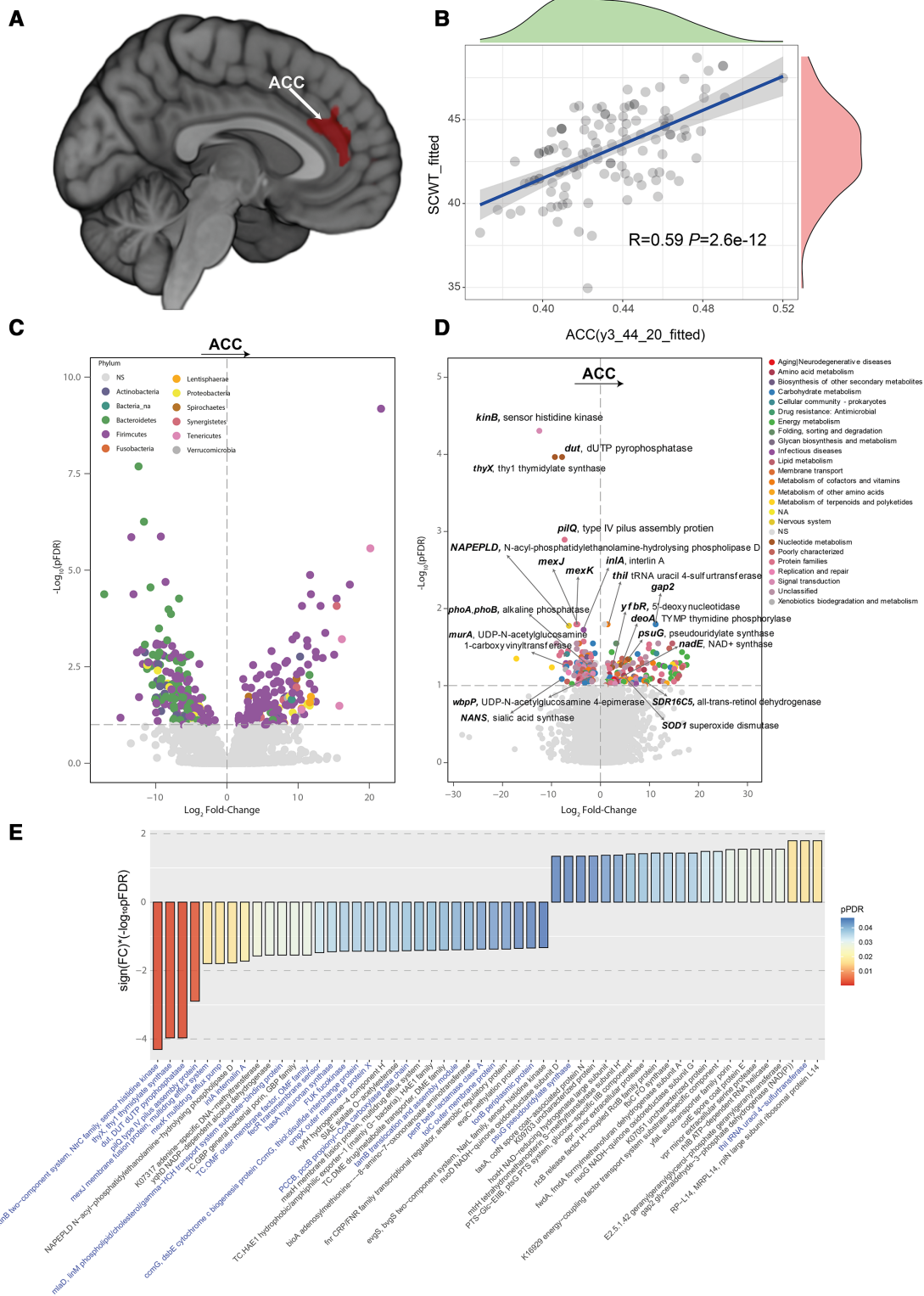
Figure 6 The gut microbiota is associated with the brain area involved in inhibitory control. (A, B) The anterior cingulate cortex (ACC) volume was positively associated with the Stroop Color and Word Test (SCWT) in the Ironmet cohort (n=95) after controlling for age, sex, education years and total intracranial volume. (C) Volcano plots of differential bacterial abundance and (D) KEGG metagenome functions associated with the ACC volume as calculated by DESeq2 controlling for previous covariates. Fold change (FC) associated with a unit change in the corresponding volumes and Benjamini-Hochberg adjusted p values (pFDR) are plotted for each taxon. (E) Manhattan-like plot of significantly expressed KEGG metagenome functions associated with the ACC volume highlighting those bacterial functions also associated with the SCWT in blue. The −log10(pFDR) values are multiplied by the FC sign to take into account the direction of the association. Bars are coloured according to the pFDR.
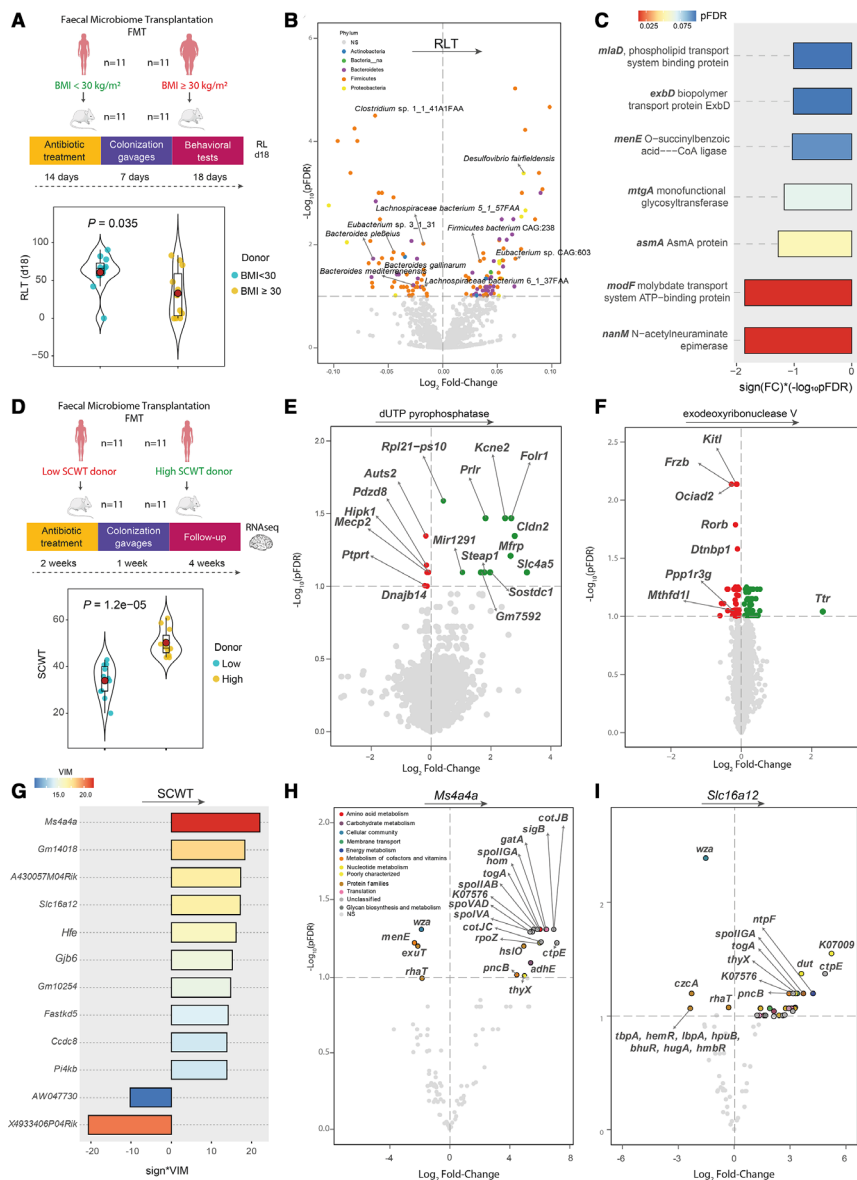
Figure 7 Faecal microbiota transplantation (FMT) mice studies. (A) Experimental design for the first FMT study. The microbiota from human donors without obesity (body mass index (BMI) <30 kg/m², n=11) and with obesity (BMI ≥30 kg/m², n=11) was delivered to recipient mice pretreated with antibiotics for 14 days. Reversal learning tests (RLT) were performed after 18 days. Violin plot for the recipient's mice RLT scores at 18 days based on human donor obesity status. (B) Volcano plot of differential human donor bacterial abundance associated with the recipient's mice RLT at day 18, identified from DESeq2 analysis controlling for donor's age, sex and education years. Fold change (FC) associated with a unit change in the corresponding memory test and Benjamini-Hochberg adjusted p values (pFDR) are plotted for each taxon. Significantly different taxa are coloured according to phylum. (C) Manhattan-like plot showing only the significantly expressed KEGG metagenome functions associated with the recipient's mice RLT (pFDR <0.1) that were also associated with the Stroop Color and Word Test (SCWT) in humans. The $-\log_{10}$(pFDR) values are multiplied by the FC sign to take into account the direction of the association. Bars are coloured according to the pFDR. (D) Experimental design for the second FMT study. The microbiota from human donors with low (n=11) and high (n=11) SCWT scores was delivered to recipient mice pretreated with antibiotics for 14 days. RNA sequencing of the medial prefrontal cortex (mPFC) was performed after 4 weeks. Violin plots for the SCWT according to the human donor scores. (E) Volcano plots of recipient's mice differential mPFC genes associated (pFDR <0.1) with the human's donor metagenome functions dUTP pyrophosphatase and (F) exodeoxyribonuclease V controlling for donor's age, sex and education years. FC associated with a unit change in the expression of the corresponding bacterial function and the Benjamini-Hochberg adjusted p values (pFDR) are plotted for each gene. (G) Bar plot of the normalised variable importance measure (VIM) for the recipient's mice mPFC genes associated with the human donor's SCWT identified by machine learning using multiple random forest-based variable selection strategy with the Boruta algorithm with 5000 trees and 500 iterations. (H) Volcano plot of differential human donor's KEGG metagenome functions associated with recipient's mice *Ms4a4a* and (I) *Slc16a12* genes. FC associated with a unit change in the expression of both genes and Benjamini-Hochberg adjusted p values (pFDR) are plotted for each metagenome function.

transporter knockout mice show impairments of short-term and long-term memory,[40] and severe deficits in cognitive function.[41] Recently, *Ms4a4a* has also been identified as a key modulator of soluble TREM2 and Alzheimer's disease risk.[42] We then used

DESeq2 to identify those SCWT-related bacterial functions that were associated with the expression of these two genes (figure 7H,I, online supplemental tables S17 and S18). Interestingly, both genes were significantly associated with *dut*

Arnoriaga-Rodríguez M, *et al*. *Gut* 2021;**0**:1–14. doi:10.1136/gutjnl-2020-323371

and *thyX*, which we had identified as the main contributors the SCWT.

Inhibitory control, a fundamental component of executive function,[2] overrules automatic intentions to directly respond to stimuli without thought.[3] We here describe multiple interactions among the gut microbiota taxonomy and functionality, and plasma and faecal-microbiota metabolites, with inhibitory control in humans with obesity that were partially transmissible to mice. This may have therapeutic implications for the disengagement of ongoing behaviours, including the suppression of impulsive food reward-related choices in subjects with obesity.[3]

Author affiliations
[1]Department of Diabetes, Endocrinology and Nutrition, Dr. Josep Trueta University Hospital, Girona, Spain
[2]Nutrition, Eumetabolism and Health Group, Girona Biomedical Research Institute (IdibGi), Girona, Spain
[3]CIBER Pathophysiology of Obesity and Nutrition (CIBEROBN), Madrid, Spain
[4]Deparment of Medical Sciences, Faculty of Medicine, University of Girona, Girona, Spain
[5]Department of Psychiatry, Bellvitge University Hospital, Bellvitge Biomedical Research Institute (IDIBELL) and CIBERSAM, Barcelona, Spain
[6]Laboratory of Neuropharmacology, Deparment of Experimental and Health Sciences, Universitat Pompeu Fabra, Barcelona, Spain
[7]Present address: Institute of Biochemistry, Life Sciences Center, Vilnius University, Saulėtekio av. 7, LT-10257 Vilnius, Lithuania
[8]Institute of Diagnostic Imaging (IDI)-Research Unit (IDIR), Parc Sanitari Pere Virgili, Barcelona, Spain
[9]Medical Imaging, Girona Biomedical Research Institute (IdibGi), Girona, Spain
[10]Neuroimmunology and Multiple Sclerosis Unit, Deparment of Neurology, Dr. Josep Trueta University Hospital, Girona, Spain
[11]Research Group on Aging, Health and Disability, Girona Biomedical Research Institute, Health Assistance Institute, Girona, Spain
[12]Institut Universitari d'Investigació en Atenció Primària Jordi Gol (IDIAP Jordi Gol), Barcelona, Catalonia, Spain
[13]Deparment of Radiology, Dr. Josep Trueta University Hospital, Girona, Spain
[14]Cardiovascular Genetics Center, CIBER-CV, Girona Biomedical Research Institute (IDIBGI), Dr. Josep Trueta University Hospital, Girona, Spain
[15]Biomedical Research Networking Center on Cardiovascular Diseases (CIBERCV), Madrid, Spain
[16]Deparment of Cardiology, Dr. Josep Trueta University Hospital, Girona, Spain
[17]Department of Neurology, Dr. Josep Trueta University Hospital, Girona Biomedical Research Institute (IDIBGI), Girona, Spain
[18]Girona Biomedical Research Institute (IdibGi), Dr. Josep Trueta University Hospital, Girona, Spain
[19]Neurodegeneration and Neuroinflammation Group, Girona Biomedical Research Institute (IdibGi), Girona, Spain
[20]Joint Investigation Unit of FISABIO and I2Sysbio, University of València and CSIC, Valencia, Spain
[21]Biomedical Research Networking Center for Epidemiology and Public Health (CIBERESP), Madrid, Spain
[22]Institute of Mathematics, École Polytechnique Fédérale de Lausanne (EPFL), Lausanne, Switzerland
[23]Red Española de Esclerosis Múltiple (REEM), Madrid, Spain
[24]Metabolic Physiopathology Research Group, Experimental Medicine Department, Lleida University-Lleida Biochemical Research Institute (UdL-IRBLleida), Lleida, Spain
[25]Institut Català de la Salut, Atenció Primària, Lleida, Spain
[26]Research Support Unit Lleida, Fundació Institut Universitari per a la recerca a l'Atenció Primària de Salut Jordi Gol i Gurina (IDIAPJGol), Lleida, Spain
[27]Hospital del Mar Medical Research Institute (IMIM), Barcelona, Spain

Twitter Joan C Vilanova @KaiVilanova and Andrés Moya @moyasimarro1

ORCID iDs
María Arnoriaga-Rodríguez http://orcid.org/0000-0002-0394-1223
Jordi Mayneris-Perxachs http://orcid.org/0000-0003-3788-3815
Oren Contreras-Rodríguez http://orcid.org/0000-0001-8922-8084
Aurelijus Burokas http://orcid.org/0000-0002-0364-3496
Rafel Ramos http://orcid.org/0000-0001-7970-5537
Ramon Brugada http://orcid.org/0000-0001-6607-3032
Joan C Vilanova http://orcid.org/0000-0003-2148-6751
Andrés Moya http://orcid.org/0000-0002-2867-1119
Lluis Ramio-Torrentà http://orcid.org/0000-0002-6999-1004
Mariona Jové http://orcid.org/0000-0001-5577-6162
Jose Manuel Fernández-Real http://orcid.org/0000-0002-7442-9323

REFERENCES
1 Harvey PD. Domains of cognition and their assessment. *Dialogues Clin Neurosci* 2019;21:227–37.

2   Yang Y, Shields GS, Guo C, *et al*. Executive function performance in obesity and overweight individuals: a meta-analysis and review. *Neurosci Biobehav Rev* 2018;84:225–44.

3   Jansen A, Houben K, Roefs A. A cognitive profile of obesity and its translation into new interventions. *Front Psychol* 2015;6:1807.

4   Arnoriaga-Rodríguez M, Fernández-Real JM. Microbiota impacts on chronic inflammation and metabolic syndrome - related cognitive dysfunction. *Rev Endocr Metab Disord* 2019;20:473–80.

5   Puig J, Biarnes C, Pedraza S, *et al*. The aging Imageomics study: rationale, design and baseline characteristics of the study population. *Mech Ageing Dev* 2020;189:111257.

6   Vioque J, Navarrete-Muñoz E-M, Gimenez-Monzó D, *et al*. Reproducibility and validity of a food frequency questionnaire among pregnant women in a Mediterranean area. *Nutr J* 2013;12:26.

7   Yu G, Wang L-G, Han Y, *et al*. clusterProfiler: an R package for comparing biological themes among gene clusters. *OMICS* 2012;16:284–7.

8   Kamburov A, Stelzl U, Lehrach H, *et al*. The ConsensusPathDB interaction database: 2013 update. *Nucleic Acids Res* 2013;41:D793–800.

9   Kursa MB, Rudnicki WR. Feature Selection with the Boruta Package. *J Stat Softw* 2010;36:1–13.

10 Degenhardt F, Seifert S, Szymczak S. Evaluation of variable selection methods for random forests and omics data sets. *Brief Bioinform* 2019;20:492–503.

11 Morris MS, Jacques PF, Rosenberg IH, *et al*. Circulating unmetabolized folic acid and 5-methyltetrahydrofolate in relation to anemia, macrocytosis, and cognitive test performance in American seniors. *Am J Clin Nutr* 2010;91:1733–44.

12 Johnson S, Wozniak DF, Imai S. CA1 *Nampt* knockdown recapitulates hippocampal cognitive phenotypes in old mice which nicotinamide mononucleotide improves. *NPJ Aging Mech Dis* 2018;4:10.

13 Murphy FC, Smith KA, Cowen PJ, *et al*. The effects of tryptophan depletion on cognitive and affective processing in healthy volunteers. *Psychopharmacology* 2002;163:42–53.

14 Walderhaug E, Lunde H, Nordvik JE, *et al*. Lowering of serotonin by rapid tryptophan depletion increases impulsiveness in normal individuals. *Psychopharmacology* 2002;164:385–91.

15 Evers EAT, van der Veen FM, Jolles J, *et al*. Acute tryptophan depletion improves performance and modulates the BOLD response during a Stroop task in healthy females. *Neuroimage* 2006;32:248–55.

16 Scholes KE, Harrison BJ, O'Neill BV, *et al*. Acute serotonin and dopamine depletion improves attentional control: findings from the stroop task. *Neuropsychopharmacology* 2007;32:1600–10.

17 Colzato LS, van den Wildenberg WPM, van Wouwe NC, *et al*. Dopamine and inhibitory action control: evidence from spontaneous eye blink rates. *Exp Brain Res* 2009;196:467–74.

18 Roesch-Ely D, Scheffel H, Weiland S, *et al*. Differential dopaminergic modulation of executive control in healthy subjects. *Psychopharmacology* 2005;178:420–30.

19 Meyer-Lindenberg A, Miletich RS, Kohn PD, *et al*. Reduced prefrontal activity predicts exaggerated striatal dopaminergic function in schizophrenia. *Nat Neurosci* 2002;5:267–71.

20 Beloborodova N, Bairamov I, Olenin A, *et al*. Effect of phenolic acids of microbial origin on production of reactive oxygen species in mitochondria and neutrophils. *J Biomed Sci* 2012;19:89.

21 Cussotto S, Delgado I, Anesi A, *et al*. Tryptophan metabolic pathways are altered in obesity and are associated with systemic inflammation. *Front Immunol* 2020;11:557.

22 Shane B. Folate and vitamin B12 metabolism: overview and interaction with riboflavin, vitamin B6, and polymorphisms. *Food Nutr Bull* 2008;29:S5–16.

23 He X, Slupsky CM. Metabolic fingerprint of dimethyl sulfone (DMSO2) in microbial-mammalian co-metabolism. *J Proteome Res* 2014;13:5281–92.

24 Ducker GS, Rabinowitz JD. One-Carbon metabolism in health and disease. *Cell Metab* 2017;25:27–42.

25 Panula P, Nuutinen S. The histaminergic network in the brain: basic organization and role in disease. *Nat Rev Neurosci* 2013;14:472–87.

26 Zhu H, Wang N, Yao L, *et al*. Moderate UV exposure enhances learning and memory by promoting a novel glutamate biosynthetic pathway in the brain. *Cell* 2018;173:1716–27.

27 Nouchi R, Takeuchi H, Taki Y, *et al*. Neuroanatomical bases of effortful control: evidence from a large sample of young healthy adults using voxel-based morphometry. *Sci Rep* 2016;6:31231.

28 Xue G, Xue F, Droutman V, *et al*. Common neural mechanisms underlying reversal learning by reward and punishment. *PLoS One* 2013;8:e82169.

29 Izquierdo A, Jentsch JD. Reversal learning as a measure of impulsive and compulsive behavior in addictions. *Psychopharmacology* 2012;219:607–20.

30 Batterink L, Yokum S, Stice E. Body mass correlates inversely with inhibitory control in response to food among adolescent girls: an fMRI study. *Neuroimage* 2010;52:1696–703.

31 Weygandt M, Mai K, Dommes E, *et al*. Impulse control in the dorsolateral prefrontal cortex counteracts post-diet weight regain in obesity. *Neuroimage* 2015;109:318–27.

32 Cho J, Yu N-K, Choi J-H, *et al*. Multiple repressive mechanisms in the hippocampus during memory formation. *Science* 2015;350:82–7.

33 Gulmez Karaca K, Brito DVC, Oliveira AMM. MeCP2: a critical regulator of chromatin in neurodevelopment and adult brain function. *Int J Mol Sci* 2019;20. doi:10.3390/ijms20184577. [Epub ahead of print: 16 Sep 2019].

34 Kim B, Choi Y, Kim H-S, *et al*. Methyl-CpG binding protein 2 in Alzheimer dementia. *Int Neurourol J* 2019;23:S72–81.

35 Silva CS, Eira J, Ribeiro CA, *et al*. Transthyretin neuroprotection in Alzheimer's disease is dependent on proteolysis. *Neurobiol Aging* 2017;59:10–14.

36 Pjetri E, Zeisel SH. Deletion of one allele of MTHFD1 (methylenetetrahydrofolate dehydrogenase 1) impairs learning in mice. *Behav Brain Res* 2017;332:71–4.

37 Glasgow SD, Ruthazer ES, Kennedy TE. Guiding synaptic plasticity: novel roles for netrin-1 in synaptic plasticity and memory formation in the adult brain. *J Physiol* 2020. doi:10.1113/JP278704. [Epub ahead of print: 03 Feb 2020].

38 Joubert BR, den Dekker HT, Felix JF, *et al*. Maternal plasma folate impacts differential DNA methylation in an epigenome-wide meta-analysis of newborns. *Nat Commun* 2016;7:10577.

39 Lev-Vachnish Y, Cadury S, Rotter-Maskowitz A, *et al*. L-Lactate promotes adult hippocampal neurogenesis. *Front Neurosci* 2019;13:403.

40 Baroncelli L, Molinaro A, Cacciante F, *et al*. A mouse model for creatine transporter deficiency reveals early onset cognitive impairment and neuropathology associated with brain aging. *Hum Mol Genet* 2016;25:4186–200.

41 Skelton MR, Schaefer TL, Graham DL, *et al*. Creatine transporter (CrT; Slc6a8) knockout mice as a model of human CrT deficiency. *PLoS One* 2011;6:e16187.

42 Deming Y, Filipello F, Cignarella F, *et al*. The *MS4A* gene cluster is a key modulator of soluble TREM2 and Alzheimer's disease risk. *Sci Transl Med* 2019;11:eaau2291.